JOURNAL OF Materials CHEMISTRY

$Zn_3In_2O_6$—crystallographic and electronic structure

Carsten Schinzer, Florence Heyd and Samir F. Matar*

Institut de Chimie de la Matière Condensée de Bordeaux (I.C.M.C.B. UPR-CNRS 9048), 87, Avenue du Docteur A. Schweitzer, F-33608 Pessac cédex, France. E-mail: matar@icmcb.u-bordeaux.fr

Received 29th January 1999, Accepted 26th April 1999

The crystal structure of $Zn_3In_2O_6$, a potential optoelectronic material, has been reinvestigated. Contrary to earlier models, Rietveld refinements on powder diffraction data show that the compound has a layered structure made of InO_2 sheets containing InO_6 edge sharing octahedra and of (Zn/In)O layers built from trigonal bipyramids. The electronic structure of the compound was investigated within the local density functional theory using the ASW method and compared to the results obtained for pure In_2O_3. A common feature of these materials is the dominance of oxygen p states and s-like states in the band structure near the Fermi level.

Introduction

The search for new materials for the applications in the field of optoelectronics and transparent electrodes has recently been oriented toward oxides such as Zn- or Sn-doped In_2O_3 with an accent on the preparation of the compounds such as $Zn_2In_2O_5$, $Zn_3In_2O_6$ or $Zn_5In_2O_8$ in thin layers deposited on different substrates by cathode sputtering.[1] The base materials In_2O_3 and ZnO are used as transparent conducting electrodes or varistors in electronic devices. The first investigations in the ZnO–In_2O_3 system were carried out on powders thirty years ago by Kasper[2] who deduced a structural model simply from relations of the lattice parameters of the different phases and proposed a sheet model consisting of subsequent A-type Ln_2O_3 and ZnO (wurtzite) structural units. A closer study of materials in this system by Cannard and Tilley[3] seemed to confirm the findings of Kasper that a series of mixed oxides $In_2Zn_nO_{n+3}$ exists with layers of the wurtzite type separated by so-called 'faults' deriving from the bixbyite structure. However, these studies were mainly based on electron microscopy and film-detected powder X-ray diffraction and there have been no complementary studies of the crystal structure including the comparison of structure factors. Systematic studies in several In_2O_3–M_2ZnO_4–ZnO systems revealed the existence of the series $InMO_3(ZnO)_m$ where M is trivalent Al,[4] Fe[5,6] or Ga.[7] In all three systems M^{3+} can usually be replaced by In^{3+} in a solid solution, but only for M = Fe or Ga in the opposite case, *i.e.* only $Fe_2O_3(ZnO)_m$ and $Ga_2O_3(ZnO)_m$ phases exist.[8,9] The observed space groups of these phases are $P6_3/mmc$ or $R\bar{3}m$ depending on whether m is even or odd, respectively. Incommensurate superstructures are observed in the case of $m > 6$ and M = In or Ga.[10] The M cation can also be one of the rare earth metal cations. However, the studies of these systems have mostly concentrated on the phase relations rather than on the crystal chemistry and little crystallographic work has been published on the existing phases. A single-crystal study on $In_2O_3(ZnO)_m$ ($m = 3$, 4 or 5) has unfortunately been limited to Weissenberg photographs in order to confirm the space group and lattice parameters.[11] The authors argue, that in analogy to single crystal studies on $LuFeO_3(ZnO)_m$ ($m = 1$, 4, 5 or 6)[12] the crystal structure of these phases consists of three different types of layers: '$InO_{1.5}$', '$(FeZn)O_{2.5}$' and 'ZnO' sheets. However, all works neglect the fact that the crystal chemistry of In^{3+} is not necessarily identical to that of Al^{3+}, Fe^{3+} or Ga^{3+}. The purpose of the present investigation is to give further insight into the crystal chemistry of the double oxide systems $In_2O_3(ZnO)_m$ with the help of Rietveld refinement. We limit our studies to the double oxide $Zn_3In_2O_6$, which has been successfully prepared and investigated.

Furthermore, to our knowledge no band-structure calculations have been published for these materials. However, access to the specific electronic features of these materials is of great relevance to develop deterministic tools for the future design of optoelectronic materials.

Sample preparation and Rietveld refinement

Stoichiometric amounts of high purity In_2O_3 and ZnO were thoroughly homogenized and mixed together. The reactions were carried out in alumina crucibles at 1200 °C during 12 h. In order to limit the loss of indium oxide, which sublimes at 850 °C, *i.e.* at a much lower temperature than ZnO, the reaction mixture was finely ground and compacted into a pellet. After reaction a regrinding of the pellet was carried out and a characterization by powder X-ray diffraction was achieved. The $Zn_3In_2O_6$ diffraction pattern was recorded on a Philips PW 3040/00 X'pert MPD system. Kα radiation from a ceramic Cu tube operated at 40 kV × 50 mA was used in a Bragg–Brentano set-up equipped with an analyzer crystal (PG). For the Rietveld refinements, the FullProf 3.1 software package[13] was used. This software allows for the estimation of the real standard deviation using different formulae; the one given by Berar[14] was used here.

The refinement was started by a profile matching run within the given space group that led to very encouraging results. The form of the peaks was modelled using the pseudo-Voigt profile function and asymmetry correction had to be introduced for reflections lying at $2\theta < 40°$. The refinements of all crystallographic parameters of the two model structures were included subsequently. The Kasper[2] model did not work well: even after freeing the position parameters, very high R values were still obtained (around 50%). The model derived from the $InFeZn_3O_6$ structure[5,6] was more successful, with the following three cationic sites (Table 1): In^{3+} on 3a, Zn and Fe on 6c(1) and 6c(2). Owing to the similar cationic radii of Zn^{2+} and In^{3+}, a statistical distribution was considered for the last two positions. This assumption proved correct: the site occupancy factor N of any of the 6c sites did not shift significantly from the values $N_{In} = 0.25$ and $N_{Zn} = 0.75$ which indicates a statistical distribution of In and Zn in a 1 : 3 ratio. The introduction of a statistical distribution of In and Zn over all cationic sites, *i.e.* including the 3a site, lead to higher R values. The ideal site occupancy factors were therefore fixed during the final phase of the refinement and isotropic thermal parameters were refined for all sites. The B values of the oxygen positions were constrained to be equal. The resulting values are in accordance with commonly observed values. The result of the final fit is

Table 1 Results of the Rietveld structure refinement on $Zn_3In_2O_6$

Atom	Position	x	y	z	B	N
In	3a	0	0	0	0.35(8)	1.00
Zn(1)	6c	2/3	1/3	0.0727(8)	0.4(1)	0.75
In(1)						0.25
Zn(2)	6c	0	0	0.1353(8)	0.54(9)	0.75
In(2)						0.25
O(1)	6c	2/3	1/3	0.025(4)	0.5(3)	1.00
O(2)	6c	0	0	0.085(4)	0.5(3)	1.00
O(3)	6c	2/3	1/3	0.140(4)	0.5(3)	1.00

Space group $R\bar{3}m$ (No. 166); lattice parameters: $a=3.3534(2)$, $c=42.51(2)$ Å. Residuals: $R_p=11.8\%$, $R_{wp}=14.8\%$, $R_{exp}=8.94\%$, $\chi^2=2.75$, $R_{Bragg}=6.01\%$. Values in parentheses give the estimated standard deviation of the last digit applying Berar's formula.[14]

shown in Fig. 1 and final values of lattice and positional parameters as well as the residuals are given in Table 1. The structural and crystal-chemical features are presented in Figs. 2 and 3, respectively and some selected bond data are reported in Table 2.

Crystal structure

The crystal structure of $Zn_3In_2O_6$ is rhombohedral. A relatively simple structural unit is repeated three times per unit cell in the c direction. The height of this stacking unit is therefore $\frac{1}{3}c_{hex}$ and the base plane of the unit is each step shifted by (1/3, 1/3) in the a,b plane, thus giving rise to the rhombohedral space group. For simplicity, only this stacking unit is represented in Fig. 2, applying the fractional coordinates from the Rietveld refinement. It is evident from the shown hexagonal set-up that a layered structure is formed with two types of layers differing in composition: one InO_2 layer is followed by four MO layers and so on. The composition of the MO layers is easily deduced from the stoichiometry: $In_2Zn_3O_6=InM_4O_6=In(In_{1/4}Zn_{3/4})_4O_6$. This matches the refined cation distribution exactly.

Fig. 3 elucidates the coordination sphere of the different cation positions in more detail. The InO_2 layer consists of slightly distorted, corner sharing InO_6 octahedra (Fig. 3a). The stacking sequence can be described by close-packed sheets of oxygen with In^{3+} in 1/2 of the octahedral interstices. The In–O distance is 2.20(8) Å, which is equal to the sum of the ionic radii (2.22 Å) within the error. The ideal octahedron is slightly distorted: O–In–O angles are 99.1(2) and 80.9(2)° between oxygen atoms of the same layer and between different layers, respectively, *i.e.* the octahedron is flattened along its trigonal axis parallel to c_{hex}.

The coordination of M in the MO layers next to the InO_2 layer is shown in Fig. 3(b). Although the coordination sphere consists of five oxygen atoms, the distance between the metal center and the O(3) atom is too large to be considered as a

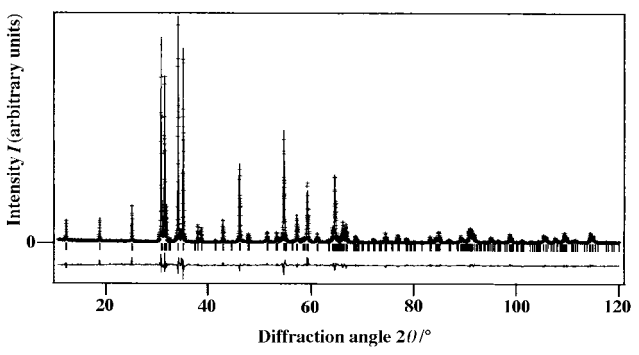

Fig. 1 Final Rietveld plot: measured (+) and calculated (—) X-ray profile, difference plot and allowed reflections as a function of diffraction angle 2θ.

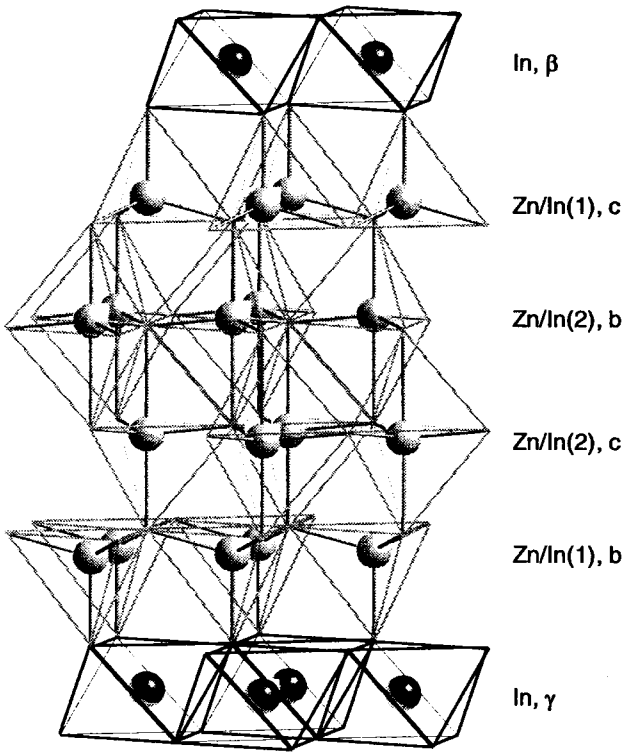

Fig. 2 Basic structural unit of $Zn_3In_2O_6$; cation positions are drawn as spheres, corners of polyhedra represent oxygen positions; characters behind the cation labels indicate octahedral (greek) and tetrahedral (roman) interstices according to the idealized structural model shown in Fig. 4 (see text).

MO bond and it is more convenient to speak of a 4+1 coordination. Regarding the distances of 2.00(4) and 2.0(2) Å to the oxygen atoms of the same layer, O(2), and to those of the InO_2 layer, O(1), respectively, a tetrahedral coordination of the In/Zn(1) site can be claimed. Moreover, the angles between the shorter bonds are 104.6(2) and 113.8(2)° for O(1)–In/Zn–O(2) and O(2)–In/Zn–O(2), respectively, not far from the ideal tetrahedral angle of 109.5°.

The situation in the MO layers far from the InO_2 layers is different. This is evident from Fig. 3(c). Three oxygen atoms, O(3), of the same layer are at 1.95(2) Å, one O(3) of the next layer is at 2.5(2) Å and one O(2) of the adjacent M(1),O layer is at 2.2(2) Å. The cation is slightly off-center by about 0.2 Å onto the M(1),O layer. Consequently, the angles O(3)–M–O(3) and O(2)–M–O(3) are 84.0(2) and 96.1(2)°, respectively. Owing to the off-centering, the intra-layer O(3)–M–O(3) angles are decreased to 118.9(2)°. It can be concluded that all surrounding oxygen atoms are involved in bonding interactions with the metal center, but with respect to the strongly varying bond lengths no coherent coordination figure can be postulated, a stretched trigonal bipyramid being the best description of the situation.

The mean distance between In/Zn and oxygen is 2.0(7) Å in the tetrahedron and 2.11(9) Å in the trigonal bipyramid. The sums of the ionic radii, based on the values given by Shannon,[15] are 1.98 and 2.07 Å, respectively, and this result is in good agreement with the experimental values. In an idealized picture, the MO sheets can therefore be regarded as constituted of wurtzite-type layers, where the ideal tetrahedral coordination is more or less distorted. Since the wurtzite structure is derived from hexagonal close packing, it is hence possible to describe the entire structure of $Zn_3In_2O_6$ by a sequence of close packed layers. This is shown schematically in Fig. 4. A, B, and C denote the three different positions of close-packed sheets, α, β, γ and a, b, c the appropriate

Table 2 Selected coordination data for $Zn_3In_2O_6$ (distances in Å, angles in °)

In–O(1)	6 × 2.20(8)	In,Zn–O(1)	1 × 2.0(2)	In,Zn–O(2)	1 × 2.2(2)
		In,Zn–O(2)	3 × 2.00(4)	In,Zn–O(3)	3 × 1.95(2)
		In,Zn–O(3)	1 × 2.9(2)		1 × 2.5(2)
O(1)–In–O(1)	80.9(2)	O(1)–In,Zn–O(2)	104.6(2)	O(2)–In,Zn–O(3)	96.1(2)
	99.1(2)	O(2)–In,Zn–O(2)	113.8(2)	O(3)–In,Zn–O(3)	118.9(2)
		O(2)–In,Zn–O(3)	75.4(2)		84.0(2)

Values in parentheses give the standard deviation of the last digit.

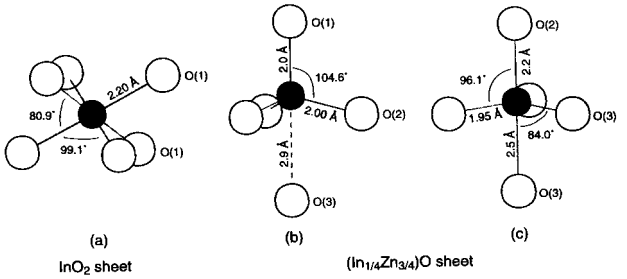

Fig. 3 Coordination of cation sites in $Zn_3In_2O_6$: (a) distorted octahedral surrounding of In in the InO_2 sheets, (b) tetrahedral and (c) trigonal-bipyramidal coordination of the metal cations in the $(In_{1/4}Zn_{3/4})O$ sheets. Standard deviations and missing values for bond angles in (b) and (c) are reported in Table 2.

octahedral and tetrahedral sites, respectively. Note that we chose the origin of our structural model in the In sheet.

The structural model proposed by Kasper is based on the observation that the hexagonal *a* parameter of $Zn_3In_2O_6$ is similar to the one observed for zincite, ZnO (space group $P6_3mc$, $Z=2$ formula units). A part of the structure of the double oxide seems thus to be imposed by that of ZnO.[2] On an increase of the Zn content, systematic changes in symmetry and an increase of the *c* parameter are observed, both explained by an elongation of the zincite-type section of the structure.[2,3] However, the assumption that the In-containing layer could be described as a part of the bixbyite-type In_2O_3 structure is not correct. Nevertheless, the similar crystal chemistry of In^{3+} and the late rare earth metal cations, especially Yb^{3+} and Lu^{3+}, whose sesquioxides all crystallize in the bixbyite type, remains the key to the structural problem.

In the papers of Kimizuka and co-workers[4–12] a structural model consisting of three different layers is applied to mixed oxides in the series $MM'O_3(ZnO)_m$ with M = Yb, Lu or In and M′ being a trivalent metal cation. The three different layers usually have different stoichiometries, namely $MO_{1.5}$, $M'ZnO_{2.5}$ and ZnO.† The layers in the Kimizuka model are made up from oxygen atoms in a close-packed arrangement with cations situated in the center of half of the triangles and subsequent layers stacked such that adjacent sheets complete the coordination sphere of the M ions to a triangular bipyramid.[12] In terms of closest packing, this implies a hexagonal stacking of the $M'ZnO_{2.5}$ and ZnO sublayers.

In the case of $Zn_3In_2O_6$ the general features found for $LuFeO_3(ZnO)_m$[12] are maintained except for the complete disorder of In and Zn on the cationic positions in the MO layers. However, the ideal configuration of the MO layers can obviously not be maintained. This is probably due to electrostatic reasons: the preference of the metal ions for trigonal-bipyramidal coordination in the MO layers arises mainly from the vicinity of the other cations. At the intersection of InO_2 and MO layers this preference is not so strong, because In^{3+} are well shielded by the surrounding oxygen atoms in the InO_2 layers, and the M cations in the layers next to these can thus move into the tetrahedral interstices. For the statistical distribution of In^{3+} and Zn^{2+} in the MO layers it has already been stated in the introduction that only few crystallographic studies have been performed and for Fe-containing materials. The considerations concerning the crystal structure of $MM'O_3(ZnO)_m$ with M = Yb, Lu or In and M′ = Al, Fe or Ga, especially the preference of M′ for the trigonal-bipyramidal coordination leading to a negligible or nil occupancy of M′ on the tetrahedral sites, are based on the assumption that the crystallographic studies are applicable without changes. Our results imply that this assumption is not necessarily valid. It is possible that the electronic configuration of the $3d^5$ cation

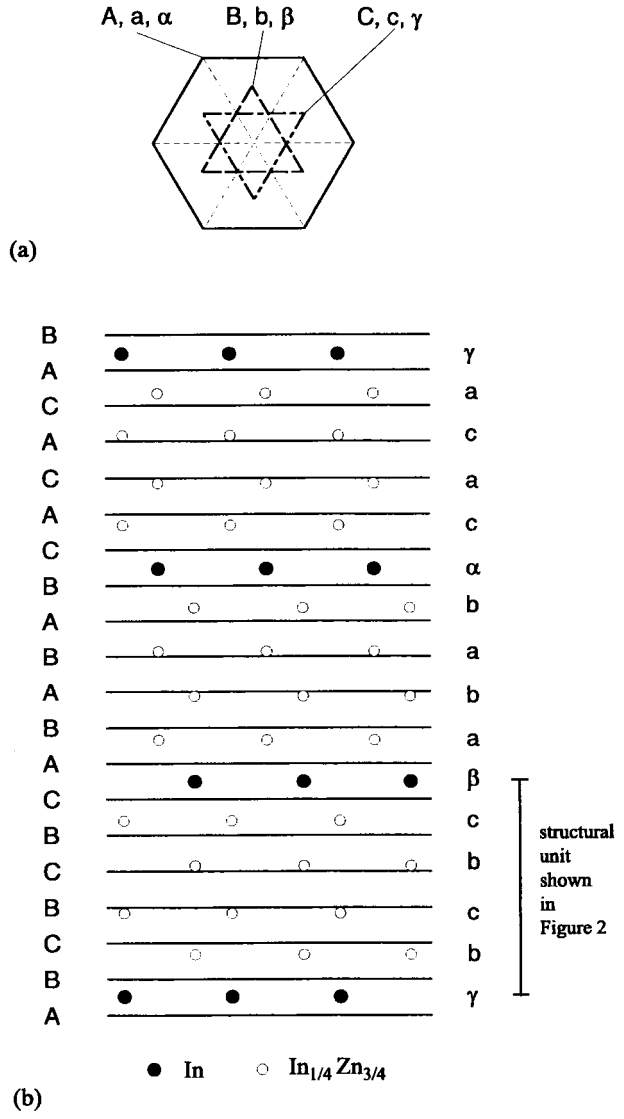

Fig. 4 Idealized stacking sequence of the structural elements in $Zn_3In_2O_6$ based on a model of closed-packed oxygen sheets (A,B,C) where cations occupy octahedral (α,β,γ) and tetrahedral (a,b,c) interstices: (a) positions of interstices in the *a*,*b* plane, (b) stacking sequence in the c_{hex} direction.

†Note that the nomenclature used by Kimizuka and co-workers is meant to be correct in terms of charge neutrality. This is the reason why they name *e.g.* the layer of octahedrally coordinated M cations '$MO_{1.5}$', where here 'InO_2' is used in order to express the composition of the structural unit.

Fe^{3+} changes due to the crystal field or that a hybridization of part of the d orbitals (e_g type ones) to form 5 σ-type bonds takes place. Both effects would lead to a preference for the trigonal-bipyramidal coordination whereas In^{3+} with a completely filled $4d^{10}$ shell behaves differently. Could Ga^{3+} ($3d^{10}$) act in a similar way as In^{3+} and could $InGaO_3(ZnO)_m$ show also a statistical distribution? This remains an open question.

$Zn_3In_2O_6$ band structure calculations

The electronic structure of the double oxide $Zn_3In_2O_6$ was approached for a hypothetical ordered structure. This is because on the one hand disorder cannot be accounted for in the framework of our calculations and on the other hand because of the large unit cell of the double oxide. The augmented spherical wave method based on density functional theory (DFT) was used in its local density approximation (LDA).[16] For exchange and correlation effects the parametrization scheme of von Barth and Hedin[17] and Janak[18] was used. In these calculations, energetically low-lying O(2s) states were considered as core states. The valence states of Zn, In (ns, np, (n−1)d; $n=4$ or 5) and O (3s, 3p) were treated as band states, therefore being part of the set of trial wavefunctions used to perform the variational procedure. However we stress here that whereas In(4d) states were accounted for as band states in pure In_2O_3, a better convergence of the calculations could be obtained when they were considered as core states and Zn(3d) as valence states in the double oxide system under consideration. This is because In(4d) lies very low in energy when In coexists with Zn in the same compound. This has been shown in a hypothetical mixed zincite structure with one Zn and one In. Using the atomic sphere approximation (ASA) and ASW method assumes overlapping spheres centered on the atomic sites. The volumes of all spheres are enforced to be equal to the cell volume. This approximation is not valid for non-compact structures as those studied here. Empty spheres (ES) were thus introduced at vacant sites in order to ensure the ASA condition and to minimize the overlap between the atomic spheres. Up to 1728 k points were used within the first Brillouin zone (BZ) to reach convergence. Self-consistency was achieved when changes of charge and total variational energy between two cycles were less than 10^{-8}. The outcome of the calculations is illustrated by the band structure and the density of states (DOS) plots given in Fig. 5. With zero energy taken at the top of the valence band (VB), the band structure along the main lines of the trigonal BZ shows an interesting feature of a nearly closing gap at the centre of the BZ (Γ) and an increasing gap away from the (Γ) point. The dispersion of the bands is also worth discussing here. Whereas it is low in the −7 to −4 eV energy window, the contrary is observed in the conduction band (CB). A simple analysis of these features is provided by the DOS plot in the lower panel of Fig. 5. The d states of In and Zn are filled by 10 electrons, hence they lie at low energy *vs.* the top of the VB. Their energy is lower than that of the O(2p) states which prevail up to the top of the VB. The high intensity peak at the top of the VB is mainly due to non-bonding O(2p) states. The large dispersion of the CB is due to s-like states arising from the In and Zn metals.

To our knowledge the electronic structure of bixbyite-type In_2O_3 has not been published yet. Before entering a discussion of the results the electronic structure of this binary compound

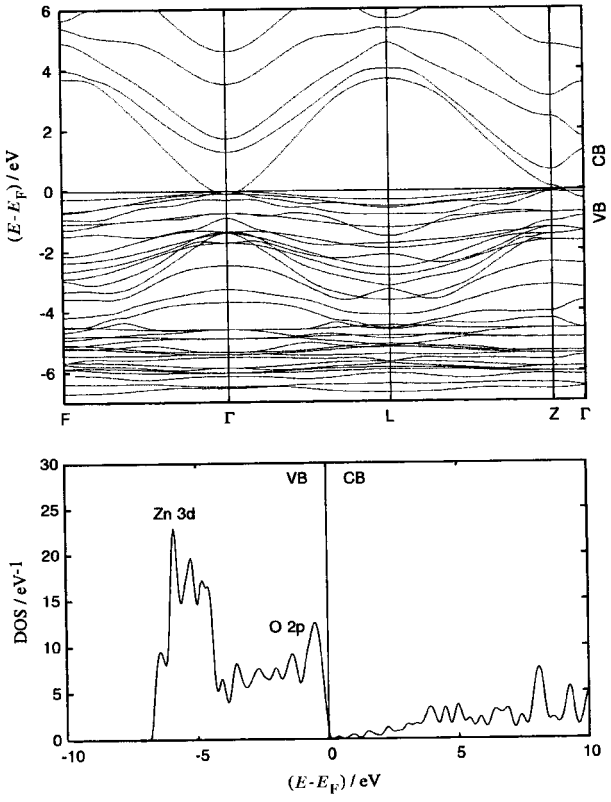

Fig. 5 Electronic structure of hypothetical $Zn_3In_2O_6$. The upper panel gives the band structure along the major directions of the Brillouin zone (BZ). Note the large band dispersion in the CB for the directions departing from the G point (center of the BZ). The lower panel shows the total DOS. Zero energy is set at the top of the VB. In(4d) states at −14 eV are not seen here. The bottom of the VB (−6 to −4 eV) is dominated by Zn(3d) states which possess a much lower dispersion than the O(2p) states that dominate the upper part of the VB. The large dispersion of s-like states at the bottom of the CB points to a free-electron-like behaviour.

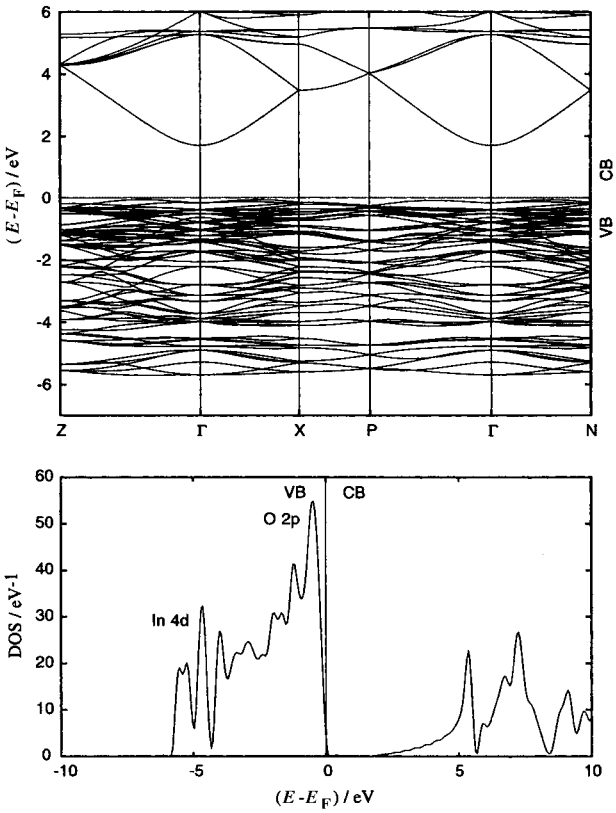

Fig. 6 Electronic structure of bixbyite-type In_2O_3. The upper panel gives the band structure along the major directions of the Brillouin zone. The band dispersion is similar to that shown in Fig. 5. The lower panel shows the total DOS. Zero energy is fixed at the top of the VB. In(4d) states lie at the bottom of the VB around −5 eV. They possess much lower dispersion than the O(2p) states that dominate up to the top of the VB. The large dispersion in the CB between 0 and 5 eV is again due to s-like states exhibiting free-electron-like behaviour.

is therefore reported. Crystallographic data were taken from Wyckoff.[19] Here, the In 4d states were considered as valence states. The band structure and DOS are presented in Fig. 6. Again, the states at the top of the VB are due to O(sp) and the dispersion of the lower CB is very high. We would stress the fact that the two calculated band structures are quite similar, although the crystal structure (rhombohedral and cubic) are not.

As stated above, an ideal ordered stoichiometry had to be assumed for the calculations, since disorder could not be accounted for. The stoichiometry had therefore to be changed to a virtual composition Zn_4InO_6. This assumption is valid because the d-valence states do not seem to play an important role. The energy of the In(4d) states (position 3a) is -14 eV in our calculation and the 3d states of Zn are situated well below the top of the VB.

As is clearly observed, the main structure of the DOS near the Fermi level does not change: a maximum near the top of the CB due to O(2p) states and the typical low-energy structure of the CB due to the high dispersion of O(2s) states is always present. These results imply that the electronic features of these materials are mainly controlled by the oxygen 2p states at the top of the VB and by s-like states arising from the metal at the bottom of the CB.

Conclusion

The crystal structure of $Zn_3In_2O_6$ has been modelled by Rietveld refinement. The structural model for this compound formerly proposed by Kasper[2] does not apply, since the conformation of the separating sheets does not represent a section of the A-type Ln_2O_3 structure as claimed by Kasper. Following the model of Kimizuka and co-workers,[11,12] the conformation of the InO_2 layers could be confirmed to be similar to the one found in the $LuFeO_3(ZnO)_m$ family, but the cationic ordering between tetrahedral (only Zn) and trigonal-bipyramidal (Zn and Fe) sites claimed by these authors could not be verified. A statistical distribution of In and Zn on both sites is found here.

The band structure calculations show clear similarities between the DOS of In_2O_3 and $Zn_3In_2O_6$, although their crystal structures are different. It is found that the band structure near the Fermi level is weakly influenced by the filled d states of the metal ions.

References

1 J. Portier, G. Campet, J. Salardenne and C. Marcel, *C.R. Acad. Sci.*, 1996, **322**, 343.
2 H. Kasper, *Z. Anorg. Allg. Chem.*, 1967, **349**, 113.
3 P. J. Cannard and R. J. D. Tilley, *J. Solid State Chem.*, 1988, **73**, 418.
4 M. Nakamura, N. Kimizuka, T. Mohri and M. Isobe, *J. Solid State Chem.*, 1993, **105**, 535.
5 N. Kimizuka, T. Mohri, Y. Matsui and K. Siratori, *J. Solid State Chem.*, 1988, **74**, 98.
6 N. Kimizuka, T. Mohri and M. Nakamura, *J. Solid State Chem.*, 1989, **81**, 70.
7 M. Nakamura, N. Kimizuka and T. Mohri, *J. Solid State Chem.*, 1991, **93**, 298.
8 M. Nakamura, N. Kimizuka and T. Mohri, *J. Solid State Chem.*, 1990, **86**, 16.
9 N. Kimizuka, M. Isobe, M. Nakamura and T. Mohri, *J. Solid State Chem.*, 1993, **103**, 394.
10 C. Li, Y. Bando, M. Nakamura, M. Onoda and N. Kimizuka, *J. Solid State Chem.*, 1998, **139**, 347.
11 N. Kimizuka, M. Isobe and M. Nakamura, *J. Solid State Chem.*, 1995, **116**, 170.
12 M. Isobe, N. Kimizuka, M. Nakamura and T. Mohri, *Acta Crystallogr., Sect. C*, 1994, **50**, 332.
13 J. R. Carvajal, FullProf, Version 3.1 for Macintosh™ PPC, 1997.
14 Yu. G. Andreev, *J. Appl. Crystallogr.*, 1994, **27**, 228.
15 R. D. Shannon, *Acta Crystallogr., Sect. A*, 1976, **32**, 751.
16 A. R. Williams, J. Kübler and C. D. Gelatt, Jr., *Phys. Rev. B*, 1979, **19**, 6094.
17 J. von Barth and D. Hedin, *J. Phys. C*, 1972, **5**, 1629.
18 J. F. Janak, *Solid State Commun.*, 1978, **25**, 53.
19 R. W. G. Wyckoff, *Crystal Structures*, Wiley Interscience, New York, 2nd edn. 1968, vol. II.

Paper 9/00790C